Deriving Molecular Parameters of Interfaces Between Chemically Identical Polymers from Macroscopically Observed Phenomena

Günter Reiter

Summary: By utilizing model systems, macroscopically observable phenomena like friction or dewetting allow to identify and to quantify molecular interfacial parameters like molecular interpenetration depth, interfacial tension, or slippage length between grafted and free chemically identical polymers. We present experimental results, which permit to extract these parameters from simple contact angle measurements or by following the dewetting process in real time with a simple optical microscope. We also show how these model experiments can provide valuable insight and fundamental understanding of processes like polymeric friction and adhesion.

Keywords: adhesion; autophobicity; dewetting; friction; polymer brush

Introduction

Interfacial phenomena are observed everywhere in our daily life.[1–3] Problems of adhesion, friction, wetting, or dewetting can be essential for the faultless performance of various applications. Intriguingly, such performance often depends on very tiny changes only. For example, the wetting behavior can be easily switched from perfect wetting to non-wetting by modifying the very surface, i.e., the last monolayer or, in some case, the end-group of the molecules at this surface.[3] Accordingly, small variations on a molecular scale can lead to dramatic effects on macroscopically observable scales.

In addition to changes in the chemical nature of the surface, properties of polymer surfaces can also be tuned by controlling the entropy of the polymer chains. If polymers are fixed to surfaces, for example, by adsorbing or grafting them onto substrates, these molecules loose some of their configurational states, i.e., they possess lower entropy.[4–9] Therefore, it is possible to obtain different behaviors at surfaces by modifying the way how polymers are attached onto surfaces.

In all the experiments presented here, we investigated exclusively the interfacial properties between chemically identical polymers. There, such interfaces are characterized by the difference in conformational entropy between end-grafted and free polymers.[4–9] Grafting polymers by one end at a high areal density onto a solid substrate leads to a reduction of the entropy of the grafted with respect to free molecules. This may lead to autophobic behavior,[4–9] i.e., the free molecules dewet the grafted layer[10–16] and form droplets on the brush.

In recent years, the basic processes involved in dewetting,[17–20] the retraction of a liquid from a non-wettable surface it was forced to cover, have been the focus of various dewetting experiments,[17,19,21–27] many of them using thin polymer films. Based on a fundamental understanding of the underlying processes, studying dewetting allows to determine interfacial properties and their changes in real time and in situ. Theoretical predictions, in particular

Institut de Chimie des Surfaces et Interfaces, CNRS-UHA, 15, rue Jean Starcky, B.P. 2488, 68057 MULHOUSE Cedex, France

by Françoise Brochard,[17–20] have been valuable guides for the design of appropriate experiments.

The static interaction between materials and wettability of materials are to a large extent characterized by the interfacial tensions. Already in 1805 Thomas Young stated[28] that contact angle measurements present a simple and surprisingly accurate way to determine molecular interactions by regarding macroscopic phenomena. However, it is difficult to investigate kinetic effects like friction (energy dissipation) at an interface by contact angle measurements alone. The necessary velocity dependent information can be obtained from dewetting experiments. Dewetting is governed by static and dynamic molecular interfacial properties. Thus, simple dewetting experiments followed by eye—or using an optical microscope for better resolution—open up possibilities to obtain time-resolved information on a molecular scale.

The dewetting experiments presented here allowed us to investigate the properties of a polymer melt slipping on a layer of chemically identical molecules. We relate the displacement of a contact line to kinetic effects at a polymer-polymer interface. As the capillary driving forces and energy dissipation at the interface are intrinsic properties controlled by molecular interactions, our system is self-adjusting at all stages of the process to any variations of experimental conditions.

Experimental Part

Samples

For our experiments, we used thin (20–850 nm) polydimethylsiloxane (PDMS) films[14–16,29,30] (liquid at room temperature) or polystyrene (PS) films[11,31] (glass transition at about 105 °C), prepared by spin coating and supported by silicon wafers which were coated with a layer of end-grafted PDMS or PS molecules.

The realization of such model systems, and in particular the fabrication of polymer brushes, either monomodal or bimodal, is schematically shown in Figure 1 for PDMS.

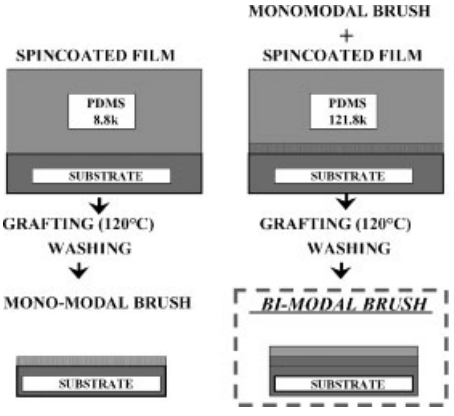

Figure 1.
Schematic drawing describing the two-step grafting process used for the preparation of bimodal polymer brushes employed as model systems for our studies.

From the dry thickness (e) of the monomodal brush ($M_w = 8\,800$ g·mol^{-1}), determined by ellipsometry, the grafting density (υ) of the brush chains, $\upsilon = e/(Na^3)$, could be deduced, with N being the number of monomers per grafted chain and a ~0.5 nm, the statistical segment length.[30] Due to the high grafting density, the chains were preferentially oriented and stretched in the direction normal to the silicon surface causing a large entropy loss of the grafted polymers.

Bimodal brushes resulted from a monomodal brush of short chains onto which we have grafted a low number Σ (per unit area) of longer PDMS chains ($M_w = 121\,800$ g·mol^{-1}). The number of grafted long chains was deduced from the difference (Δe) between the thicknesses of the dry monomodal and bimodal brushes using the following equation $\Sigma = \Delta e/Za^3$, with Z being the number of monomers of the long grafted chains.

More details can be found in ref.[14,30] for PDMS and in ref.[11,31] for PS.

Elastomeric Lenses

Drops of PDMS network were made from vinyl-terminated PDMS chains with average molecular weight of 9 400 g·mol^{-1}.[29,30]

Cross-linking was effected via hydrosilation. The spherical shape was obtained by cross-linking a PDMS drop at the end of a capillary tube giving radii of curvature between 1 and 2 mm. Swelling experiments in toluene revealed an average mesh size, M_c, between 6 000 and 10 000 $g \cdot mol^{-1}$, i.e., the number of monomers between cross-linked points, N_c, ranged from 81 to 135. The cross-linked PDMS drops were only used after extraction of the free chains.

Dewetting Measurements

We measured the displacement of the front (Fr) and the rear (Re) position of the rim as a function of time (Figure 2) using optical microscopy.[14,15] The starting point of zero distance (O) was set by breaking the silicon substrate along a crystallographic axis in two parts. By breaking the sample, we created a three-phase contact-line between the substrate, the film, and the surrounding environment (mostly air purged with nitrogen), which represented the starting point for dewetting. The dewetted distance (d) is given by $d(t) = Fr(t) - O$ and the width of the rim (w) is given by $w(t) = Re(t) - Fr(t)$. From these measures, we obtained the dewetting velocity (V) by taking differences: $V(t_i) = [d(t_i) - d(t_{i-1})]/(t_i - t_{i-1})$. A typical result is shown in Figure 3.

Friction Measurements

Friction measurements were performed with a pin-on-disc device[29,30] (high temperature tribometer from CSEM) schematically shown in Figure 4. The tangential force, F, induced a deflection of the force sensor, which was transformed into an electrical voltage proportional to the friction force. Weights mounted at the end of the beam above the slider are applied to produce the normal load. A low load (8 g) was selected, just high enough to ensure that the network drop stayed in contact with the substrate. Temperature, radial frequency, and radius of friction track (2 mm) were controlled. The corresponding linear velocity ranged from 15 $\mu m \cdot s^{-1}$ to 130 $mm \cdot s^{-1}$. The force was recorded continuously. The contact area (A) was determined in real time by a CCD camera.

Theoretical Considerations[17–20]

In a typical dewetting experiment, the driving capillary forces F_d (uncompensated Young force) are balanced by viscous forces F_v (forces per unit length of the

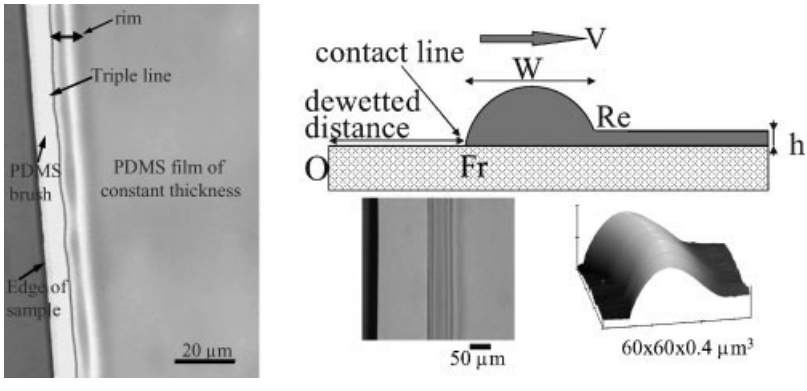

Figure 2.
Left: Typical optical micrograph showing dewetting of a thin PDMS film from the edge of a sample. Right: Schematic representation of the experimental set-up. A typical shape of the rim, which is built up in the course of dewetting, as measured by atomic force microscopy, is shown in the lower right corner. Note that the lateral scale is about a factor of 100 larger than the vertical scale. On the left to the AFM image, we show an optical micrograph representing the top view corresponding to the scheme. The spacing between successive interference fringes is somewhat smaller on the left side indicating a steeper slope. This is confirmed by the cross-section of the AFM image on the right. The contact angle determined directly by AFM or obtained from the spacing of the interference fringes agrees nicely with the values obtained from Equation (2) (see later).

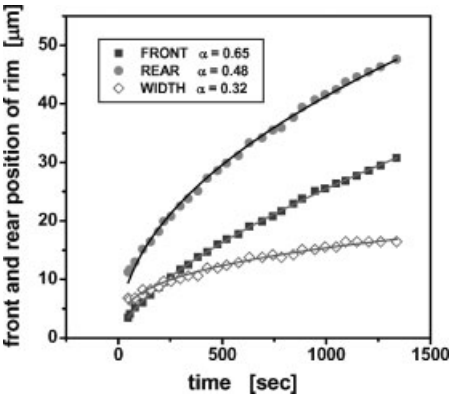

Figure 3.
Dewetting of a PDMS film (92 nm, $M_w = 308\,000$ g · mol^{-1}) on top of a densely grafted brush of end-functionalized PDMS molecules (brush thickness: 6.3 nm, $M_w = 8\,800$ g · mol^{-1}). The temperature was $T = 50\,^{\circ}$C. The front (Fr) and rear (Re) positions of the rim as a function of time are shown by the squares and circles, respectively. The position of the origin (O) has been set to zero. The width (w) of the rim is given by open diamonds. The full lines are best fits to the data using the following equation: $Y = C^{st} \cdot (t - t_o)^{\alpha}$, where Y stands for Fr, Re, and w, respectively. C^{st} is a constant prefactor and t_o is the time-offset. Results for the exponent α are given in the inset. For all our experiments at low temperatures around 50 °C we obtained (within the error-bar of about 0.05) exponents $\alpha = 2/3$ and $\alpha = 1/3$ for the temporal increase of d and w, respectively.

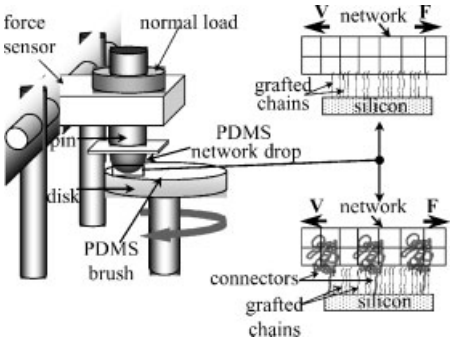

Figure 4.
Schematic view of the tribometer used in this study. The pin is touching the disk at chosen distance away from the rotation axis of the disk. Schematic illustrations of the interface between the network and a monomodal brush (top panel) or a bimodal brush (bottom panel) are shown on the right part of the figure.

three-phase contact line): $F_d = F_v$. In a good approximation, F_d is determined by the contact angle (θ) and the surface tension (γ) of the liquid: $F_d = 0.5 \cdot \gamma \cdot \theta^2$. F_v depends on the hydrodynamics of liquid retraction on top of the substrate. For non-slipping films, the energy is dissipated in a small volume located at the contact line. Then, F_v is simply proportional to the viscosity (η) and the velocity (V). In such dewetting experiments, V has to be constant in time.[17] However, long polymers on a non-adsorbing substrate have been found to slip.[14,15,19] In such cases, the energy is dissipated over the whole moving part of the film characterized by the width (w) of the rim collecting the liquid from the dewetted region. There, $F_v = 3 \cdot \eta \cdot V \cdot w/b$. The parameter b is called the slippage length.

$$F_d = 0.5 \cdot \gamma \cdot \theta^2 = 3 \cdot \eta \cdot V \cdot w/b = F_v \quad (1)$$

For non-volatile liquids like polymers, w is related to the dewetted distance (d) by mass conservation. For a film of thickness (h) we obtain

$$d \cdot h = C \cdot w^2 \cdot \theta \quad (2)$$

The constant C (~0.1) accounts for the asymmetric shape of the rim.[18] We want to point out that Equation (2) allows to determine the contact angle at any stage of the dewetting experiment.

Equation (1) and (2) provide for the time (t) dependence of d, w, and V the following equations:

$$d(t) = A \cdot t^{2/3}$$

$$w(t) = B \cdot t^{1/3}$$

$$V(t) = 2/3 \cdot A \cdot t^{-1/3} \quad (3)$$

with the prefactors A and B, assumed to be time-independent, being

$$A = (0.25 \cdot \gamma \cdot C^{1/2})^{2/3} \cdot \theta^{5/3} \cdot b^{2/3} \cdot \eta^{-2/3} \cdot h^{-1/3} \quad (4a)$$

$$B = (0.25 \cdot \gamma \cdot C^{-1})^{1/3} \cdot \theta^{1/3} \cdot b^{1/3} \cdot \eta^{-1/3} \cdot h^{1/3} \quad (4b)$$

Measuring the width of the rim at time t_i and determining the velocity from the temporal increase of d, we get b directly without any fitting [i.e., without the use of Equation (3)] for any time interval $(t_i - t_{i-1})$. This opens up the possibility to check for possible temporal changes in b. In particular, we do not have to assume any exponent for a power-law relation between d and t.

$$b(t_i) = \frac{3 \cdot \eta \cdot V(t_i) \cdot w(t_i)}{F_d(t_i)} \quad (5a)$$

Using A and B obtained from fits [based on Equation (3)] to the curves of d and w as a function of time, respectively, (i.e., assuming that b and θ do not depend on time) we get:

$$b = \frac{2 \cdot \eta \cdot A \cdot B}{F_d} \quad (5b)$$

Results and Discussions

Autophobic Behavior of Polymers

Experimentally, the surface tension γ of a liquid is usually found to decrease with increasing temperature, implying an increase of the excess interfacial entropy (ΔS). In the case of autophobicity, an interfacial tension is created between identical molecules. When polymers are attached to a surface, e.g., by permanently grafting these molecules at one end to the substrate, theory expects a reduction of the interfacial entropy rather than an increase when a melt penetrates a grafted polymer layer (polymer brush). The penetration and the wettability of grafted (or adsorbed) polymers by the melt of identical molecules are quite important phenomena by themselves in the context of adhesion and friction or the compatibilization of polymer blends using block copolymers. In particular, it is relevant to know if wettability, adhesion, or compatibility improve (positive ΔS) or decrease (negative ΔS) at elevated temperatures. The phenomenon of autophobicity becomes clearly visible in both, static and dynamic systems, i.e., droplets of a polymeric liquid or the dewetting of a polymer film on its own monolayer. Contact angle measurements allow to determine the interfacial γ_{MB} tension between melt and brush, as we show below in Figure 5–7 for PDMS droplets.[16]

From $\theta(T)$ we determined the interfacial tension $\gamma_{MB}(T)$ between the melt and the brush for different temperatures using the following relation, based on Young's equation and assuming that the melt and the brush have about the same surface tension.[4,32]

$$\gamma_{MB}(T) = \gamma_{LV}(T)[1 - \cos\theta(T)] \quad (6)$$

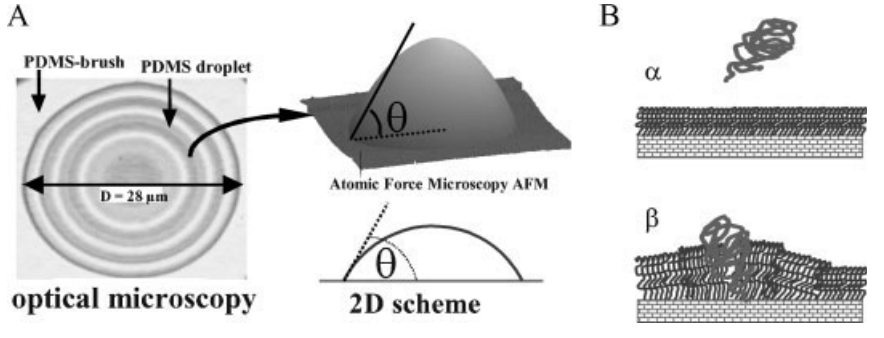

Figure 5.
Part A: Optical microscopy image of a small PDMS droplet on a PDMS brush. The white light interference (Newton) rings reflect the contact angle θ, which was also measured by AFM. The scheme below shows how θ was determined. Part B: Cartoon to illustrate (α) the steric (entropic) problems when an incoming extra polymer chain will encounter (β), it penetrates the already rather dense polymer brush in order to get grafted to the substrate.

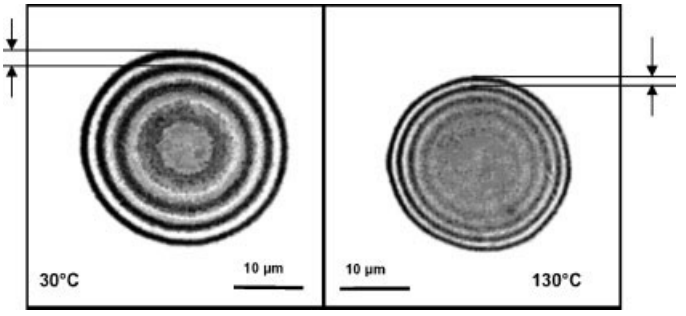

Figure 6.
Typical optical micrographs showing the influence of temperature on the contact angle θ for the studied melt-brush system. The droplet, obtained by dewetting, was photographed at 30 and 130 °C, respectively. The interference fringes become narrower as temperature increases. The change in θ and the interfacial tension (γ_{MB}) between melt and brush after 1 h equilibration at 130 °C are: $\Delta\theta = 2.3 \pm 0.2^{\circ}$ and $\Delta\,\gamma_{MB} = +30 \pm 1.3\ \mu N \cdot m^{-1}$.

For the temperature dependence of the surface tension of the melt (γ_{LV}) we used the results found by Sauer and Dee:[32] $\gamma_{LV} = C_1 + C_2 T$, with $C_1 = 22.05\ mN \cdot m^{-1}$ and $C_2 = -60\ \mu N \cdot m^{-1} \cdot {}^{\circ}C^{-1}$.

Within experimental uncertainties due to contact angle hysteresis and systematic errors in the contact angle measurements, all our experiments indicate that, extrapolating our results to lower temperatures, $\gamma_{MB}(T)$ tends to zero at absolute zero temperature. Noting that $d[\gamma_{MB}(T)]/dT = \Delta S_{MB}$, $\gamma_{MB}(T = -273\ {}^{\circ}C) \sim 0\ N \cdot m^{-1}$ implies that the interfacial tension is of purely entropic origin, corroborating that the brush-coated wafers do not allow for enthalpic interactions (e.g., adsorption).

The excess surface entropy ΔS_{surf} of a PDMS melt was found to be positive and of the order of $+60\ \mu N \cdot m^{-1} \cdot {}^{\circ}C^{-1}$.[32] Here, for the excess interfacial entropy ΔS_{MB} between PDMS brush and PDMS melt, we

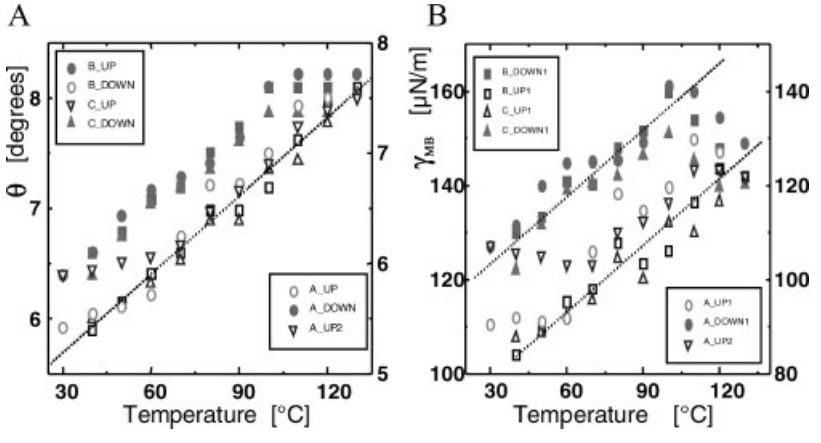

Figure 7.
Influence of temperature (T) on contact angle θ and interfacial tension γ_{MB} for three (A, B, C) PDMS droplets with diameters between 20 and 50 µm residing on PDMS brushes. A: θ and (B) γ_{MB} as a function of increasing (open symbols) and decreasing (full symbols) T. The droplets were equilibrated at each temperature until no further changes could be detected. Usually this took about 5 min. Due to slight differences in the absolute values we had to use different y-axis (left axis for droplets B and C). The dotted lines serve as guides to the eye. Note the pronounced hysteresis and the fluctuations around the dotted lines, which we attribute to contact line pinning.

found a value about two orders of magnitude lower. Furthermore, and even more importantly, the value of ΔS_{MB} was negative, as expected theoretically. This means that from the entropy point of view it is better to keep melt and brush separated than to bring them in contact, although both consist of chemically identical molecules.

Determining Contact Angle and Slippage Length from Dewetting Experiments[14,15]

In order to be as close as possible to the assumptions made by theory, in particular a non-adsorbing interface, we have chosen the polymer brush-melt system described above which avoided specific interactions between different chemical species. As explained before, measuring the dewetted distance and the width of the rim simultaneously allowed us to determine the contact angle in situ and in real time based on the assumption of mass conservation [see Equation (2)]. Typical results are shown in Figure 8. It should be noted that, due to small differences in the brush properties, the value of the contact angle differed between samples but it was rather constant in time. In spite of this high sensitivity on conditions of preparation, most of the studied samples showed values within a narrow band from 4 to 10°.[14]

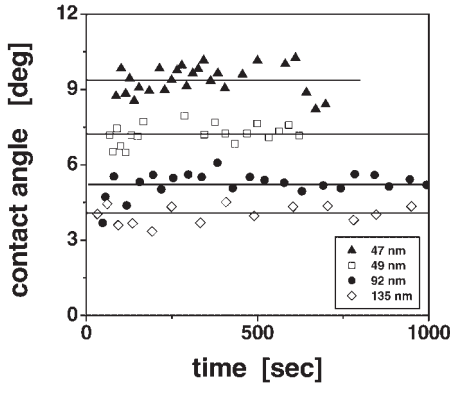

Figure 8.
Contact angles as determined from Equation (2) for various films dewetting the underlying PDMS brush at $T = 50\ ^{\circ}C$ as a function of time. The films have the following thicknesses: 47 nm (triangles), 49 nm (squares), 92 nm (circles), and 135 nm (diamonds). The lines represent guides to the eye. For almost all our samples θ(t) turned out to be constant or only slightly decreasing (about 10%) in time.

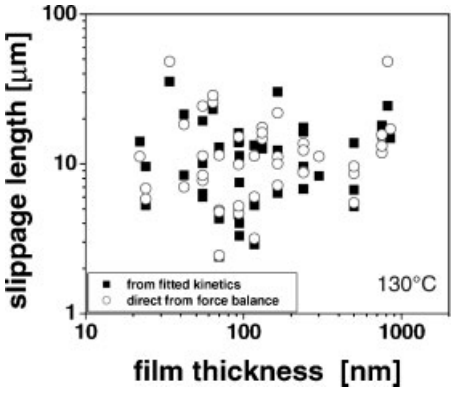

Figure 9.
Slippage length as determined from Equation (5a), averaged over the whole time range of the experiment (open circles), and deduced from the prefactors A and B (full squares) using Equation (5b) as a function of film thickness on double logarithmic scales. Data were obtained at $T = 130\ ^{\circ}C$.

We could determine the dewetting velocity, the width of the rim, and the driving force (i.e., the contact angle) independently. This allowed us to use both Equation (5a) and (5b) to determine the slippage length for our system. Both ways yielded very similar results. The results for $T = 130\ ^{\circ}C$ are shown in Figure 9. It should be noted that our samples did not allow to find a clear relation between contact angle and slippage length.[14]

We want to emphasize that we have determined and varied all relevant parameters independently. η was varied by taking different monodisperse polymer fractions or by performing experiments at different temperatures, the values of γ are tabulated[32] and do not vary much for the molecular weights of the chosen polymers, θ was determined from mass conservation [Equation (2)] and b from the balance of viscous and capillary forces [see Equation (1)]. Consequently, our macroscopic dewetting experiments allowed us to obtain time-resolved information on interfacial

properties like the slippage length or the dynamic contact angle. In addition, all other relations between the above parameters can be found, e.g., the velocity dependence of b or the relation between the friction coefficient k and θ. We note that, in contrast to most other dewetting experiments, we were measuring the dewetted distance and the width of the rim simultaneously. This allowed us (1) to test theory and (2) to determine contact angle and slippage length, even without any fitting or the ''guess'' of additional parameters.

We want to draw the attention to the fact that the observed slippage length was quite large (of the order of 10 μm). b is related to the friction coefficient k (per area a^2 of a monomer) by $k = \eta/b$. A comparison between a typical value for k obtained in our experiments and the value of the monomeric friction coefficient[33] $k_o = 3.7 \times 10^7$ Pa · s · m^{-1} shows that only a few (x) frictional contacts (per unit interfacial area) contributed to the measured friction ($k = x \cdot k_o$). This implies that the free molecules could penetrate only very little into the densely grafted brush.[4,16] Less perfect brushes of slightly lower grafting density showed lower θ and much lower b, i.e., deeper interpenetration.

We also want to add a word of caution, which at the same time shows the high sensitivity of our approach. Although we prepared rather excellent polymer brushes (a necessary pre-requisite for the autophobic behavior in first place: ''bad'' brushes, i.e., brushes of low or heterogeneous grafting density, did not show dewetting at all) our samples differed nonetheless somewhat, expressed by different contact angles and slippage lengths. Thus, these values have to be determined for each sample individually. Without knowing the exact values of θ and b, one cannot determine the correct thickness dependence of the prefactors A and B and may erroneously question theory. Consequently, only after having determined these two parameters (θ and b) one can compare the behavior of different samples, even if these samples have been prepared exactly the same way and even if the thickness of the grafted layer was constant within the resolution of ellipsometry (0.2 nm). The difference in dewetting behavior between samples does not result from inaccurate measurements as demonstrated by repeated measurements on the same sample, which give the same results.

The parameters θ and b characterize static and kinetic interfacial properties, respectively. These two parameters can vary independently. Samples with the same contact angle may exhibit rather different values of b. As we show later in this paper, adding a few connector molecules (the same as the brush molecules but of higher molecular weight) to a polymer brush can significantly slow down (or even stop) dewetting.[31] However, as long as the number of these connector molecules is low, no measurable change in the contact angle could be detected.

Comparing Friction Coefficients Obtained by Dewetting and Independent Friction Experiments[29,30]

In order to compare our results obtained in dewetting studies with results from ''classical'' friction experiments, we have also performed measurements with a standard tribometer. Figure 10 shows the friction force F per unit area A (i.e., F/A) as a function of sliding (drive) velocity V_S for two different substrates. We can distinguish two qualitatively different behaviors. The first is a quasi velocity-independent friction for systems where molecules at one surface were immobile and could not penetrate the PDMS network (hydrophobic silicon wafers coated with a chlorodimethylvinylsilane monolayer (Si-CDMVS)). This behavior is well known for elastomers sliding on solid surfaces.[34]

The second type of behavior showed a more pronounced velocity dependence of friction and concerns PDMS coatings. At the lowest velocities, these systems exhibited significantly lower friction (though increasing with velocity) whereas at the highest velocities such systems behaved

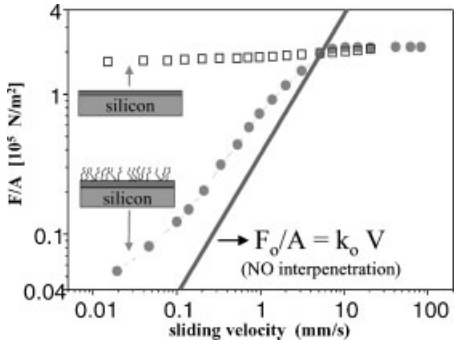

Figure 10.
Variation of the shear stress F/A with sliding velocity V_S for two different substrates: □, silicon wafer coated with CDMVS and ●, monomodal brush of short chains ($e = 6.6$ nm, $M_w = 8\,800$ g·mol^{-1}, $\Sigma = 0.44$ chains·nm^{-2}). The thick solid line represents the calculated value of F/A for a network sliding, on a planar surface of monomers, using $(F/A)_{MONOMER} = (\zeta_1/a^2) \cdot V$ with $\zeta_1 =$ taken from ref.[33]

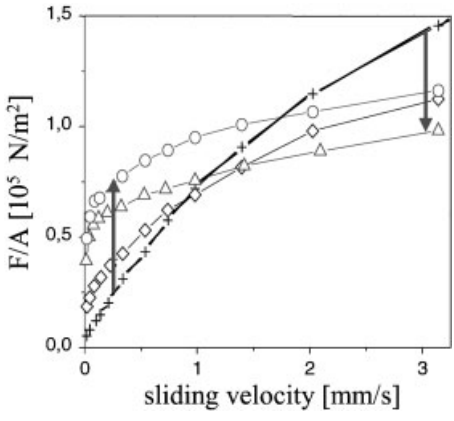

Figure 11.
Variation of F/A with V_S for different numbers (Σ) of connectors (per unit area). +, $\Sigma = 0$ (monomodal brush, $M_w = 8\,800$ g·mol^{-1}); ◇, $\Sigma = 0.0068$; □, $\Sigma = 0.016$; Δ, $\Sigma = 0.027$; ○, $\Sigma = 0.094$ connectors·nm^{-2}. The mesh size of the network is 6 600 g·mol^{-1}.

like solid substrates. These two regimes were separated by a transition zone with quite important fluctuations of the friction force.[30] The solid line in Figure 10 gives the calculated friction expected for a planar smooth interface of monomers according to $(F/A)_{MONOMER} = (\zeta_1/a^2) \cdot V$, using the value of $\zeta_1/a^2 = 3.7 \times 10^7$ Pa·s·m^{-1} given in ref.[33] At low velocities, our measured values are higher than $(F/A)_{MONOMER}$. This can be attributed to a frictional contribution of more monomers than contained in a planar interface. Consequently, we assume that there is a small penetration of some brush monomers into the network, which, however, decreased to about zero at the point where the measured value of F/A and $(F/A)_{MONOMER}$ became equal and the network started to slide on top of the ''solid-like'' brush surface. We note that the velocity at this transition is comparatively low. In spite of obvious differences in the experimental approach, the results obtained for sliding a PDMS network on a PDMS brush fully corroborate our conclusions drawn from dewetting of a PDMS melt on a PDMS brush.

The behavior of bimodal brushes with respect to friction is presented in Figure 11. There, the number of long chains fixed within the densely grafted brush of much shorter polymers is always comparatively low. These long polymers are able to penetrate into the elastomer and are thus acting as ''connectors.'' Naively, one expects that such connectors make it more difficult to slide the elastomer over the brush surface, i.e., the presence of long chains should increase friction. However, comparing a mono-modal brush of short chains (little interpenetration) with bimodal brushes of controlled number of connectors, we observed two opposing trends. At the lowest sliding velocities, adding connectors increased friction, consistent with observations by Brown.[33] This has to be contrasted to the behavior at higher velocities where the same connectors led to a reduction of friction, even below the value of $(F/A)_{MONOMER}$. Such a lubrication effect (within a certain velocity window) is surprising because it is not (yet) expected by theory. However, it has to be noted that theory did not consider in detail how the extracted connectors interact with each other and how this intercalated layer of strongly deformed polymers affects friction. Our experimental results clearly show

that such a layer can act as an effective lubricant.

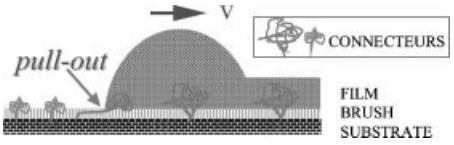

Figure 12.
Schematic drawing of a moving rim of a thin film on a dense polymer brush driven by capillary forces and competing against pull-out forces due to "connector" molecules. Brush, connectors, and film are made from some type of polymer.

Determining the Force per Polymer Chain Necessary to Pull it out of its own Melt[31]

As mentioned in the "Introduction," tiny changes at interfaces can provoke rather dramatic consequences. In the above experiments, we have used rather simple and well-defined model systems of polymer brushes of short molecules grafted at a sufficiently high grafting density to cause autophobic behavior. In many cases, however, polymers are not grafted to surfaces but they are rather physically adsorbed. In a first approximation such an adsorbed layer can be considered as a brush but consisting of polymer chains having different lengths ("pseudo-brush"). In the next step of approximation, we have reduced such a pseudo-brush to a bimodal brush consisting of two chain lengths only. We modeled such bimodal brushes systematically by anchoring a controlled number of long chains into the brush of short chains. As shown in Figure 12, these long chains act also as "connectors" in dewetting, similar to the friction experiments described above. We expect that dewetting can be stopped and films can be stabilized when a sufficiently high number of connectors are grafted onto the brush.

In Figure 13, we present results from dewetting studies where we varied the area-density of connectors systematically. These experiments were performed with PS, but similar results have also been obtained for PDMS. Our results demonstrate quite nicely that even at relatively low grafting density, e.g., one connector per 1 000 nm^2 for connectors of 126 $kg \cdot mol^{-1}$, a significant reduction in dewetting velocity can be observed. Based on such systematic studies,

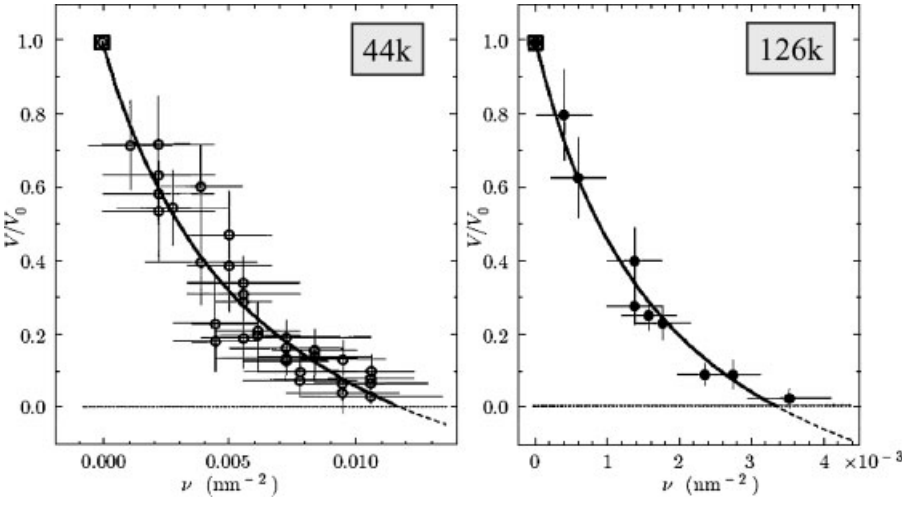

Figure 13.
Dewetting velocity (V) of PS ($M_w = 43\ kg \cdot mol^{-1}$) on PS brushes ($M_w = 9\ kg \cdot mol^{-1}$), normalized by the velocity (V_0) without connectors, as a function of area-density of connectors (ν) for (a) $M_w = 44\ kg \cdot mol^{-1}$ and (b) $M_w = 126\ kg \cdot mol^{-1}$ connectors. The solid lines represent a fit to the data based on a model described in detail in ref.[31]

we were able to obtain (by extrapolation) the minimal density of connectors, which is needed to stop dewetting. It becomes clear that this density is significantly lower for the longer connectors than for the shorter ones.

In the following we attempt to explain this behavior based on the molecular mechanisms involved. The motion of the rim is determined by the balance of driving capillary forces (F_d), diminished by the resisting pull-out forces (F_p) due to the connectors, and the viscous forces (F_v) (all forces are per unit length of the contact line): $F_d - F_p = F_v$.

Assuming that the curvature of the rim is constant, F_d is approximately $0.5\ \gamma\theta^2$, with θ being the static contact angle and γ the surface tension of the melt.

The total resisting pull-out force is proportional to ν times the distance (L) the connectors are stretched during the pull-out process (all connectors within L experience a force):

$$F_p \sim \nu L f^* \quad (7)$$

f^* is the pull-out force per chain, which results from two effects.[35] The chains do not want to be exposed to air. As they resist being pulled out they get stretched, which reduces their entropy.

In the limit of $V \to 0$ (no dewetting), $F_d = F_p$ and thus we can obtain $f^* = \nu L/F_d$. Taking into account that at maximum a connector can be pulled by the contact line over its full length (i.e., $L = Na$), we get $f^* = \nu Na/F_d$. From our experiments, we obtain that f^* is about 3×10^{-13} N. As expected from above considerations and theory, this value does not depend on the molecular weight of the connectors used.

Conclusions

From the results presented here we can clearly and unambiguously conclude that polymers cannot only dewet but even slip on their own brush as a consequence of autophobicity. Moreover, our polymer systems are ideally suited for testing theoretical predictions of the consequences of slippage in dewetting. From measures of the dewetted distance and the width of the rim collecting the retracted liquid we determine in a straightforward way the "incompatibility" between free and grafted identical molecules, expressed by the contact angle, and the interfacial friction characterized by a slippage length. The theoretically predicted relations between velocity, energy dissipation, capillary driving force, viscosity, and film thickness have been successfully verified. Based on these relations, we also have access to an interpretation of the changes in interfacial properties in the course of the experiment, impossible for any other technique of such simplicity. In addition, detailed information about polymeric friction and adhesion can be obtained. Thus, dewetting experiments provide a practical and fast means for interfacial characterization, both static and dynamic.

In summary, it is not always necessary to employ sophisticated techniques to access molecular parameters, an optical microscope may be sufficient. Of course, model systems like the ones used here, which allow to precisely control relevant parameters and which permit clear observations, form the basis of such experiments. Then, even rather "cheap" experiments provide a profound insight into processes at molecular scales. The examples mentioned here clearly demonstrate this possibility.

[1] P. G. De Gennes, F. Brochard-Wyart, D. Quéré, "*Gouttes, Bulles, Perles et Ondes*", Belin, Paris 2002.
[2] P. G. de Gennes, *Rev. Mod. Phys.* **1985**, *57*, 827.
[3] J. N. Israelachvili, "*Intermolecular and Surface Forces*", 2nd edition, Academic Press, 1991.
[4] L. Leibler, A. Ajdari, A. Mourran, G. Coulon, D. Chatenay, in: *Ordering in Macromolecular Systems*, A. Teramoto, M. Kobayashi, T. Norisuje, Eds., Springer-Verlag, Berlin **1994**, p. 301.
[5] K. Shull, *Faraday Discuss.* **1994**, *98*, 203.
[6] C. Gay, *Macromolecules* **1997**, *30*, 5939.
[7] P. G. Ferreira, A. Ajdari, L. Leibler, *Macromolecules* **1998**, *31*, 3994.
[8] M. W. Matsen, J. M. Gardiner, *J. Chem. Phys.* **2001**, *115*, 2794.
[9] M. Müller, L. G. MacDowell, *Europhys. Lett.* **2001**, *55*, 221.
[10] Y. Liu, et al., *Phys. Rev. Lett.* **1994**, *73*, 440.

[11] G. Reiter, P. Auroy, L. Auvray, *Macromolecules* **1996**, *29*, 2150.
[12] G. Henn, D. G. Bucknall, M. Stamm, P. Vanhoorne, R. Jérôme, *Macromolecules* **1996**, *29*, 4305.
[13] S. Sheiko, E. Lermann, M. Möller, *Langmuir* **1996**, *12*, 4015.
[14] G. Reiter, R. Khanna, *Langmuir* **2000**, *16*, 6351.
[15] G. Reiter, R. Khanna, *Phys. Rev. Lett.* **2000**, *85*, 2753.
[16] G. Reiter, R. Khanna, *Phys. Rev. Lett.* **2000**, *85*, 5599.
[17] C. Redon, F. Brochard-Wyart, F. Rondelez, *Phys. Rev. Lett.* **1991**, *66*, 715.
[18] F. Brochard-Wyart, P. Martin, C. Redon, *Langmuir* **1993**, *9*, 3682.
[19] C. Redon, J. B. Brzoska, F. Brochard-Wyart, *Macromolecules* **1994**, *27*, 468.
[20] F. Brochard-Wyart, G. Debrégeas, R. Fondecave, P. Martin, *Macromolecules* **1997**, *30*, 1211.
[21] G. Reiter, *Phys. Rev. Lett.* **1992**, *68*, 75.
[22] P. Lambooy, K. C. Phelan, O. Haugg, G. Krausch, *Phys. Rev. Lett.* **1996**, *76*, 1110.
[23] G. Krausch, *J. Phys.: Condens. Matter* **1997**, *9*, 7741.
[24] K. Jacobs, S. Herminghaus, J. R. Mecke, *Langmuir* **1998**, *14*, 965.
[25] G. Debrégeas, P.-G. de Gennes, F. Brochard-Wyart, *Science* **1998**, *279*, 1704.
[26] J. Masson, P. Green, *Phys. Rev. Lett.* **2002**, *88*, 205504.
[27] R. Seemann, S. Herminghaus, K. Jacobs, *Phys. Rev. Lett.* **2001**, *87*, 196101.
[28] T. Young, *Philos. Trans. R. Soc. London* **1805**, *95*, 65.
[29] A. Casoli, M. Brendlé, J. Schultz, P. Auroy, G. Reiter, *Tribology Lett.* **2000**, *8*, 249.
[30] A. Casoli, M. Brendlé, J. Schultz, P. Auroy, G. Reiter, *Langmuir* **2001**, *17*, 388.
[31] G. Reiter, J. Schultz, P. Auroy, L. Auvray, *Europhys. Lett.* **1996**, *33*, 29.
[32] [32a] B. B. Sauer, G. T. Dee, *J. Coll. Interface Sci.* **1992**, *152*, 85; [32b] B. B. Sauer, G. T. Dee, *Macromolecules* **1991**, *24*, 2124.
[33] H. R. Brown, *Science* **1994**, *263*, 1411.
[34] B. N. J. Persson, "*Sliding Friction: Principles and Applications*", Springer, Heidelberg, **1998**.
[35] E. Raphaël, P.-G. de Gennes, *J. Phys. Chem.* **1992**, *96*, 4002.

